VOLUME 118 July 2012 ISSN: 0375-6742

JGE

JOURNAL OF
GEOCHEMICAL
EXPLORATION

JOURNAL FOR ENVIRONMENTAL AND ECONOMIC GEOCHEMISTRY

http://www.elsevier.com/locate/jgeoexp

Journal of Geochemical Exploration 118 (2012) 98–110

Contents lists available at SciVerse ScienceDirect

Journal of Geochemical Exploration

journal homepage: www.elsevier.com/locate/jgeoexp

Delineation of mineralization zones using concentration–volume fractal method in Pb–Zn carbonate hosted deposits

Seyed Taghi Delavar [a,*], Peyman Afzal [b], Gregor Borg [c], Iraj Rasa [d], Mohammad Lotfi [e], Nematolah Rashidnejad Omran [f]

[a] Department of Geology, Science and Research Branch, Islamic Azad University, Tehran, Iran
[b] Department of Mining Engineering, South Tehran Branch, Islamic Azad University, Tehran, Iran
[c] Martin-Lutherr-University Halle – Wittenberg, 06120 Halle, Germany
[d] Earth Sciences Faculty, Shahid Beheshti University, Tehran, Iran
[e] Department of Geology, North Tehran branch, Islamic Azad University, Tehran, Iran
[f] Department of Geology, Tarbiat Modares University, Tehran, Iran

ARTICLE INFO

Article history:
Received 20 July 2011
Accepted 6 May 2012
Available online 17 May 2012

Keywords:
Mineral resource exploration
Mineralization zones
Pb–Zn carbonate hosted deposits
Concentration–volume (C–V) fractal model
Tangedezan, Iran

ABSTRACT

This study uses the C–V fractal model to separate mineralization zones especially enriched supergene and hypogene protore in an Iranian Pb–Zn carbonate hosted deposit, based on subsurface data. The Tangedezan deposit is located in central Iran. In order to separate the two major mineralization zones in this deposit, log–log plots of major elements are prepared, which are fitted straight lines that show C–V relationship for Pb, Zn, Ag and Cd especially in NE of the area. Based on power–law relationship between elemental concentrations and their host rock volume, the oxidation and sulfidation zones are separated. Log–log plots for the mentioned elements show three mineralization zones including enriched supergene (oxidation), hypogene sulfide protore and low mineralization zones. The obtained results were compared with geological zonation model. This comparison shows that the interpreted zones by the C–V fractal model are in agreement with the proposed geological model. The C–V log–log plot for Zn reveals that there is an enriched supergene zone (oxidation), which separates out at the Zn grade of 13.8% in Tangedezan deposit. The high sulfide zone (hypogene protore) interpreted to have 7.2% to 13.8% and the low mineralization zone, mainly consisting of low sulfidation and to lesser extent low oxidation, has less than 7.2% of Zn grade in the deposit.

1. Introduction

Separation of enriched supergene (oxidation) and hypogene protore and low sulfidation is one of the main goals in exploration of Pb–Zn carbonate hosted deposits (e.g., Reichert and Borg, 2008). Different customized methods for zone detection and separation in this type of deposits are usually based on geological parameters such as mineralographical, petrographical, geological structures and alterations, specifically in dolomitization and silicification types (e.g., Bradley and Leach, 2003; Ghazban et al., 1994; Leach et al., 2010; Meyer, 1981; Reichert and Borg, 2008; Sangameshwar and Barnes, 1983; Takahashi, 1960). Historically, applicable models used for recognition of different mineralization zones in Pb–Zn carbonate hosted deposits have been based on understanding of the fundamental controls such as geochemical environments (Hutchinson, 1992; Leach et al., 2001, 2010; Meyer, 1981; Sangster, 1990; Sawkins, 1984).

Several scientists focused on separation of different mineralization zones in carbonate hosted Pb–Zn deposits and divided these deposits to oxidation and sulfidation zones (Leach et al., 2001; Sangster, 1996; Shelton and Hagni, 1993). Others worked on non-sulfide carbonate hosted Pb–Zn and identified the emplacement of non-sulfide ore generally subdivided into an 'oxidation stage' followed by a 'post-oxidation stage' (Reichert and Borg, 2008).

One important and reliable data that helps to separate the mineralization zone is the borehole data especially if it has a logging information including mineralographical information, alteration and host rock changes. Different geological interpretations could be presented for detecting zone boundaries, which may also lead to different results because the elemental grade distribution may not be taken into consideration.

The fractal theory is one of the non-linear mathematics that was established by Mandelbrot (1983) and widely applied by geoscientists (e.g., Afzal et al., 2010, 2011; Agterberg et al., 1993; Ali et al., 2007; Cheng et al., 1994; Goncalves et al., 2001; Li et al., 2003; Shen and Zhao, 2002; Sim et al., 1999; Turcotte, 1986; Zuo et al., 2009). Methods based on fractal geometry can investigate relationships between geological, geochemical and mineralogical settings with spatial

---

* Corresponding author. Tel.: +98 912 3359536.
E-mail address: stdelavar@yahoo.com (S.T. Delavar).

0375-6742/$ – see front matter © 2012 Elsevier B.V. All rights reserved.
doi:10.1016/j.gexplo.2012.05.003

information derived from data analysis (Afzal et al., 2011; Carranza, 2008, 2009).

As quantitative thresholds can be recognized and determined in the plot's breaking points, various log–log plots in fractal methods are suitable tools for separation of geological and geochemical populations. These investigations proposed that fractal method can be applied to investigate the separation within mineralization zones in various types of deposits.

Based on the Zn, Pb, Ag and Cd grades, and using of concentration–volume (C–V) fractal method, distinguishing the enriched supergene (oxidation), hypogene sulfide protore and low mineralization (low sulfidation and oxidation) zones, is the main aim of this research in the Tangedezan Pb–Zn carbonate hosted deposit located in Central Iran.

2. Concentration–volume fractal method

Afzal et al. (2011) proposed the fractal concentration–volume (C–V) model for separating various mineralization zones in order to characterize the distribution of major, minor and trace element concentrations in relation to the Iranian Cu porphyry deposits (Sungun and Chah-Firuzeh). This model has the general form:

$$\boldsymbol{V}(\boldsymbol{\rho} \leq \boldsymbol{\upsilon}) \propto \boldsymbol{\rho}^{-\boldsymbol{a}1}; \boldsymbol{V}(\boldsymbol{\rho} \geq \boldsymbol{\upsilon}) \propto \boldsymbol{\rho}^{-\boldsymbol{a}2} \qquad (1)$$

where, $V(\rho \leq \upsilon)$ and $V(\rho \geq \upsilon)$ denote volumes (V) with concentration values (ρ) that are, respectively, smaller and greater than contour values (υ), which define those volumes, and a1 and a2 are exponents. In the log–log plots of concentration contours versus volumes, certain concentration contours representing breakpoints in the plots are considered threshold values separating geochemical populations in the data (Afzal et al., 2011). To calculate $V(\rho \leq \upsilon)$ and $V(\rho \geq \upsilon)$ enclosed by a concentration contour in a 3D model, in this study, the original borehole data of ore element concentrations were interpolated by using the inverse distance weighted (IDW) method.

Breakpoints between straight-line segments in those log–log plots represent threshold values separating populations of geochemical concentration values representing mineralization zones according to distinct geochemical processes. In the Pb–Zn carbonate hosted deposits, zones of high Zn, Pb, Ag and Cd concentrations comprise relatively few voxels in a 3D block model, whereas zones low of these elemental concentrations comprise numerous voxels. Therefore threshold values in this recognized by applying the fractal C–V method likely represent boundaries between different ore zones.

3. Geological setting of the case studies

High amounts of zinc and lead are produced from Pb–Zn carbonate hosted in the world (Alldrick and Sangster, 2005). About 600 Zn–Pb deposits and occurrences are prospected in Iran by now

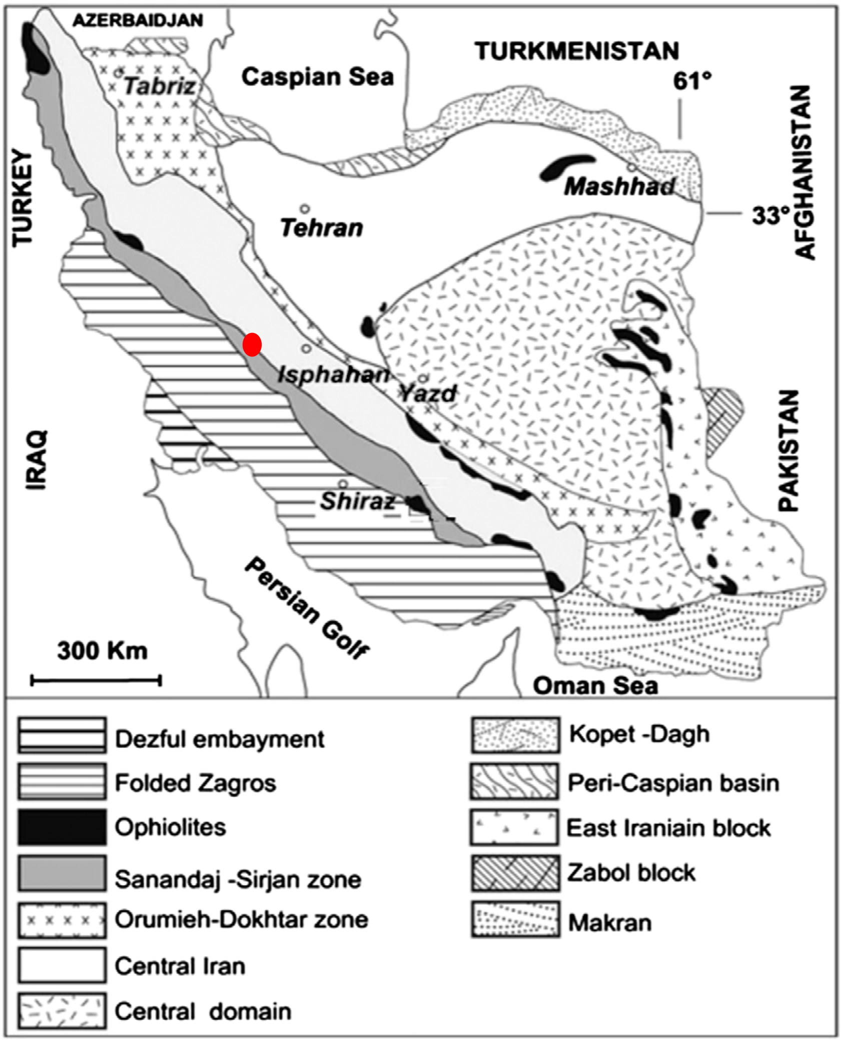

Fig. 1. Location of Tangedezan deposit in Sanandaj–Sirjan zone in structural map of Iran (Alavi, 1994).

(Ehya et al., 2010; Ghorbani et al., 2000). The most important metallogenic provinces for Pb–Zn mineralization are in Central Iran, the Sanandaj–Sirjan Zone, and the Alborz region (Ghazanfari, 1999; Meshkani et al., 2011), as depicted in Fig. 1. The ages of the mineralization events and host rocks range from the Upper Proterozoic to Oligocene–Miocene; however, most of the host rocks are either Paleozoic or Cretaceous carbonates (Ehya et al., 2010; Reichert, 2007).

The Pb–Zn deposits are common in the Sanandaj–Sirjan Zone by 1500 km long, up to 200 km wide, and extend from northwest to southeast Iran, especially in its middle part, the Malayer–Esfahan belt, where it is predominantly stratabound and restricted to Cretaceous limestones, dolomites, shales, and occasionally sandstones, although some deposits have pre-Cretaceous host rocks (Meshkani et al., 2011; Momenzadeh, 1976). Sulfidic mineralization and non-sulfide ores are dominant in this belt. The proposed hypotheses for the origin of these deposits vary from MVT to Sedex models (Ghorbani, 2002; Reichert, 2007). The subduction of the Neo-Tethyan ocean floor beneath Iran sutured Iran to Arabia, e.g., Alavi (1994), and the subsequent continental convergence built the Zagros orogenic belt including Sanandaj–Sirjan belt (Ghasemi and Talbot, 2006; Sheikholeslami et al., 2003).

The Tangedezan deposit is situated about 160 km NW of Isfahan city in the Malayer–Esfahan belt, as illustrated in Fig. 1. The sulfide and non-sulfide ores of Tangedezan are hosted in Cretaceous carbonates (Thiele et al., 1968). There is a stratabound deposit that concluded oxidation zone in surface and sulfidation zone in depth. Geologic map of the Tangedezan area (1:20,000 scale) is shown in Fig. 2. The host rock dominantly thrust on adjacent units. Faults and other structural features (fold and lamination) with dominant NW–SE trends parallel to the Zagros orogen are the major structural features in the Tangedezan area. The ore in the oxidation zone is mainly composed of hemimorphite, smithsonite and cerussite and in the sulfidation zone sphalerite and galena existed and pyrite, calcite, dolomite quartz and barite are gangue minerals. The major wall-rock alteration observed in the deposit comprises dolomitization and silicification. Dolomitization has increased the effective porosity and permeability for the precipitation of mineralization.

4. C–V fractal model in the Tangedezan deposit

The Tangedezan deposit data were obtained from 17 drill cores covering a total length of about 1100 m. Rock samples from the drill cores were used to construct the zonation model based on geological core logging and 330 lithogeochemical samples with 2 m interval from drill cores in the this deposit were analyzed by ICP-OES for Zn, Pb, Ag and Cd and 39 other elements. The Tangedezan deposit is modeled with 433,980 voxels. Each voxel has a dimension of 2 × 2 × 2 m in the X, Y and Z directions. Zn, Pb, Ag and Cd distribution block models were generated via inverse distance squared (IDS) method using the RockWorks 15 software package (RockWare Co.,

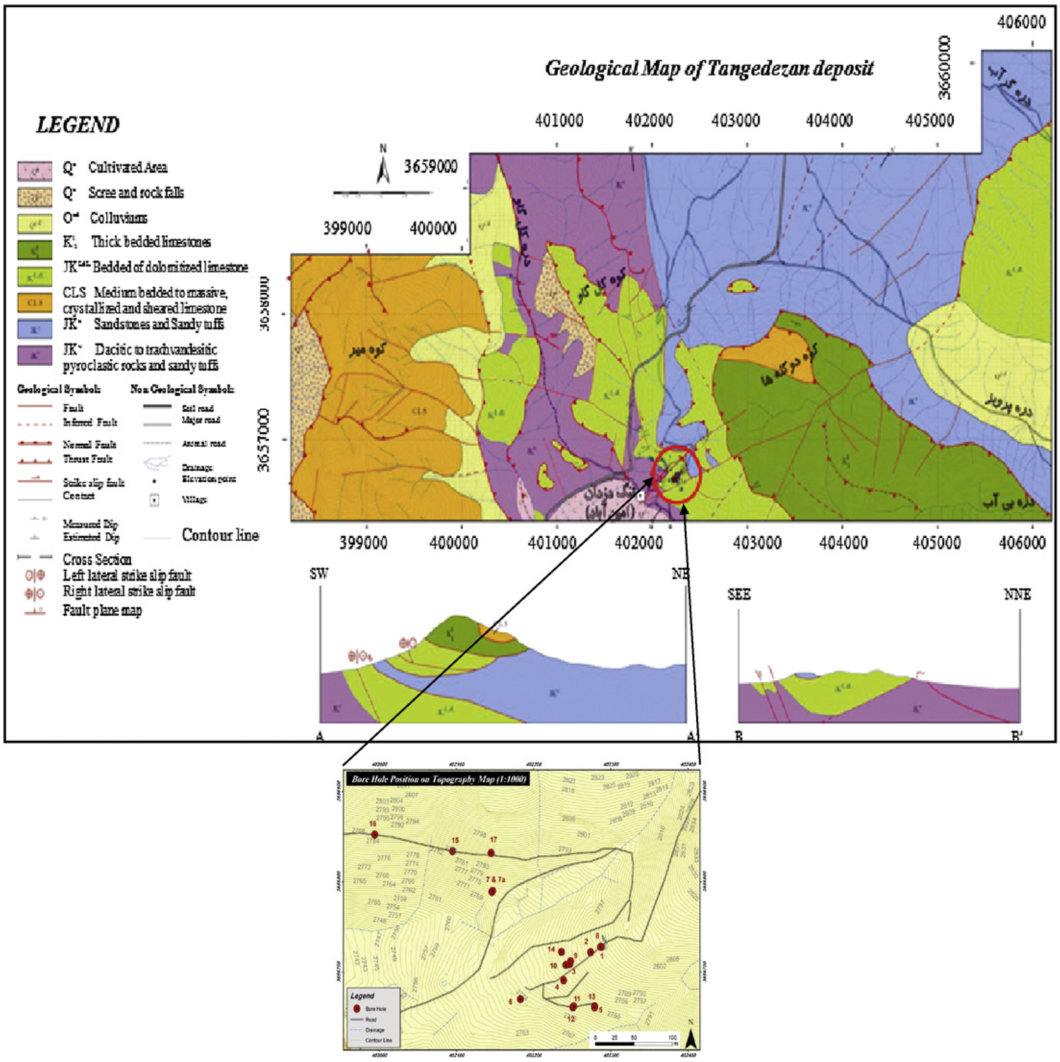

Fig. 2. Geological map of Tangedezan deposit in1:20,000 scale (Parsgostaran Co., 2010).

2010). To calculate V(ρ ≤ υ) and V(ρ ≥ υ) enclosed by a concentration contour in a 3D model, in this study, the original drill core data of ore element concentrations were interpolated by using the inverse distance squared (IDS) method. Volumes V(ρ ≤ υ) and V(ρ ≥ υ) are equal to the unit volume of a voxel (or volume cell) multiplied by the number of voxels with concentration values (ρ) that are, respectively, smaller and greater than a certain concentration value (υ).

Elemental thresholds values were identified from log–log plot (Fig. 3). It demonstrates a power–law relationship between Zn, Pb, Ag and Cd concentrations and volumes occupied. Geochemical populations for these elements are separated by different straight-line segments in the log–log plots. The fitted lines were determined by least squared law in Excel software. All elemental log–log plots show three geochemical populations that occurred in this area. There is a sudden change in the rate of decrease of the volume enclosed by high values of Zn, Pb, Ag and Cd, as depicted in Fig. 3. However, the slope of the segments is close to 90° that shows enriched population in geochemical exploration (Cheng et al., 1994). Based on the log–log plot, Zn concentrations in enriched supergene zone are considered to range higher than 13.8%. Above 3%, 62 ppm and 407 ppm lies an enriched supergene zone based on Pb, Ag and Cd log–log plots, respectively (Table 1).

The second populations of the mentioned elements can be interpreted as hypogene sulfide protore zone with a concentration range between 7.2% and 13.8% for Zn and range between 1.66% and 3% for Pb. Also, in hypogene sulfide protore zone of this deposit Ag and Cd respectively range between 30 and 62 ppm and 52 and 407 ppm (Table 1).

The first elemental geochemical populations could be described as low mineralization zone. Based on geological observations most parts of this mineralization zone show low sulfidation and less low oxidation in this deposit. Lower than the first threshold from the left of the graphs is about 7.2%, 1.66%, 30 ppm and 52 ppm respectively for Zn, Pb, Ag and Cd which is interpreted to be the threshold of background for the ore element of this deposit.

The results of the C–V method for the mentioned elements have been shown in Fig. 4. The third geochemical populations (enriched supergene) in the log–log plot generated as 3D models of elemental distribution in this deposit by using RockWorks 15 software package, as presented in Fig. 4. All of the third geochemical populations of these elements are situated in Eastern and NE part of this deposit, especially Zn and Pb. In addition, Ag higher than 62 ppm and Cd higher than 407 ppm are extended in other parts of Tangdezan deposit (Fig. 4). According to these models a high oxidation zone (enriched

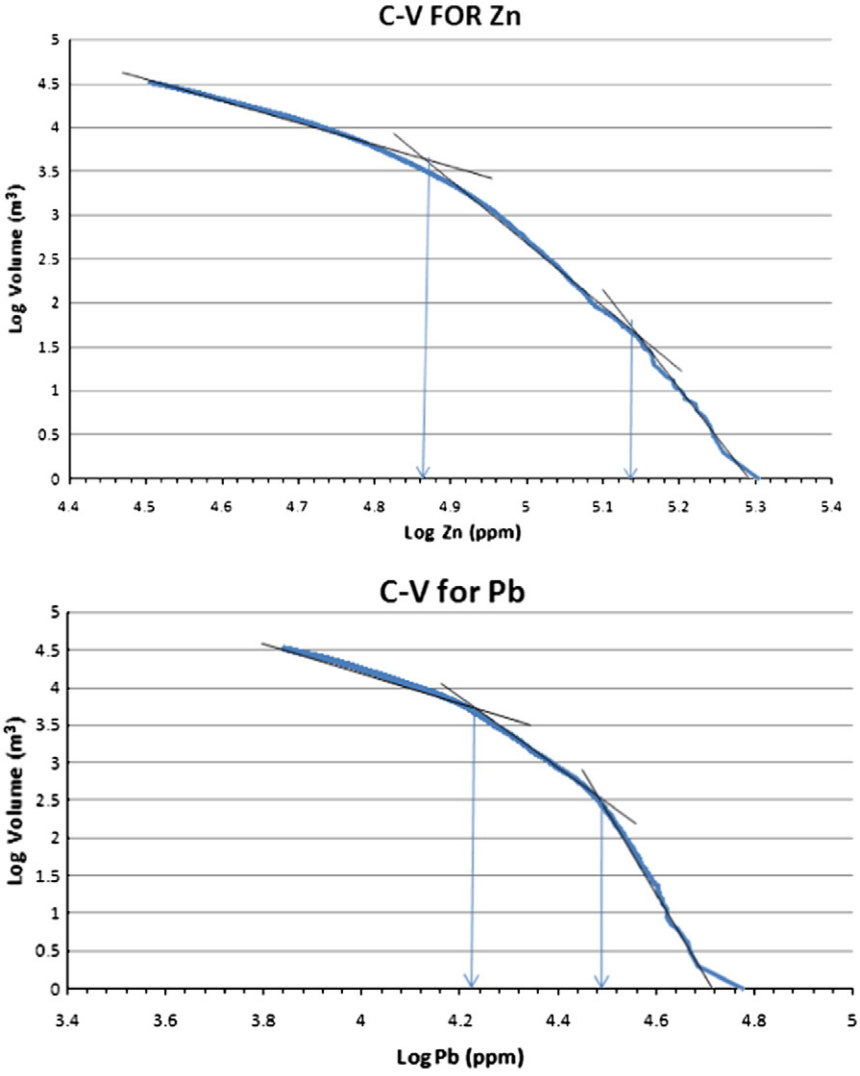

Fig. 3. C–V log–log plots for Zn, Pb, Ag and Cd.

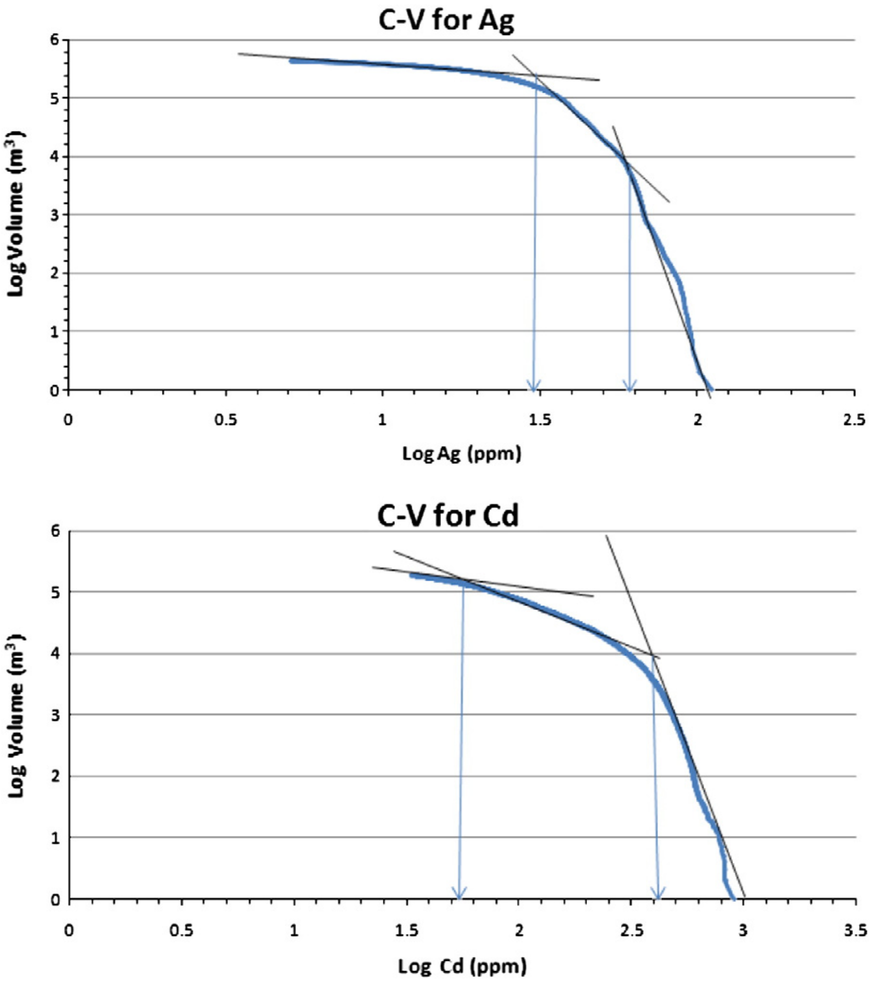

Fig. 3 (*continued*).

supergene) is situated near the surface and it is located in the E–NE part of the area.

The second geochemical populations of Zn, Pb, Ag and Cd are located in the NE, northern and NW parts of this deposit, as presented in Fig. 5. It is obvious that the mineralization zone occurred in depth and shows that there are hypogene sulfide protore mineralizations for these elements since elemental grade ranges are proper and economical. Ag between 30 and 62 ppm and Cd between 52 ppm and 407 ppm occurred in deeper parts of this deposit (Fig. 5). The geochemical populations lower than the first elemental thresholds could be interpreted as low mineralization zone in Fig. 6. The low mineralization zone occurred in most parts of the deposit. Based on 3D models presented in Fig. 6, most parts of this zone concluded low sulfidation mineralization. But there are low intensity oxidation zones that can be interpreted as transition zone between oxidation and sulfidation mineralization. Moreover, there are barren host rocks, which show no obvious evidence of mineralization outside of the low mineralization zone based on geological studies.

Comparison between geological data and results obtained from C–V method were made by construction of zonation model of the Tangdezan deposit base on geological logging from drilling data, as depicted in Fig. 7. Enriched supergene zone resulting from the C–V method is correlated with the E–NE part of the oxidation zone obtained by geological zonation model. Additionally, the oxidation zone derived by geological model in northern and NW parts of the area is correlated with Ag and Cd enriched supergene zone in terms of C–V fractal model. There are no sufficient drilling data and could be interpreted that enriched supergene for Zn and Pb will be proposed to be explored in future program. Hypogene sulfide protore zone obtained from the C–V model is correlated with hypogene sulfide protore zone from the geological zonation model in eastern and N–NW parts of the deposit especially in depth, as illustrated in Fig. 7. There is a good correlation between low mineralization zone from the C–V method and low sulfidation zone from the geological zonation model, as depicted in Fig. 7. This shows that parts of the low mineralization zone obtained by C–V model are correlated within the oxidation zone derived via geological zonation model in north part of the deposit. It can be interpreted that several parts of oxidation zone from drilling data are transition zones between oxidation and sulfidation mineralization.

5 . Conclusions

In this paper, concentration–volume (C–V) fractal method is applied for the separation of different mineralization zones in Pb–Zn

Table 1
Elemental ranges for resulting zones from C–V model.

Zone	Range (Zn%)	Range (Pb%)	Range (Ag ppm)	Range (Cd ppm))
Low mineralization zone	<7.2	<1.66	<30	<52
Hypogene protore zone	7.2–13.8	1.66–3	30–62	52–407
Enriched supergene zone	>13.8	>3	>62	>407

carbonate hosted in Tangedezan deposit, central Iran. Based on interpretation of log–log plots of major and minor elements of this deposit including Zn, Pb, Ag and Cd, there are three major mineralization zones including enriched supergene, hypogene sulfide protore and low mineralization zones. Low mineralization zones consist of high amounts of low sulfidation zone and lower intensity oxidation and

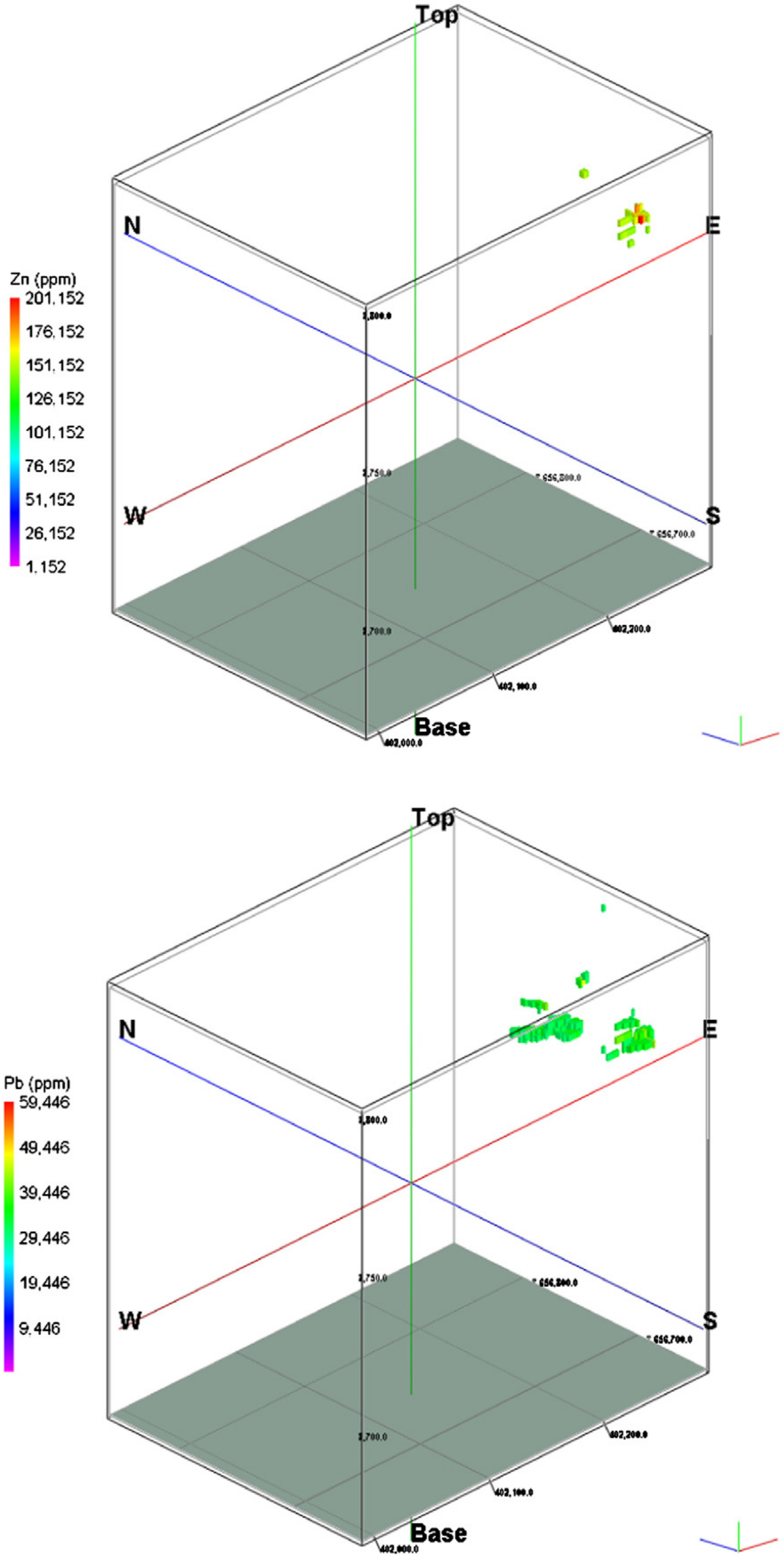

Fig. 4. Enriched supergene zone based on C–V method.

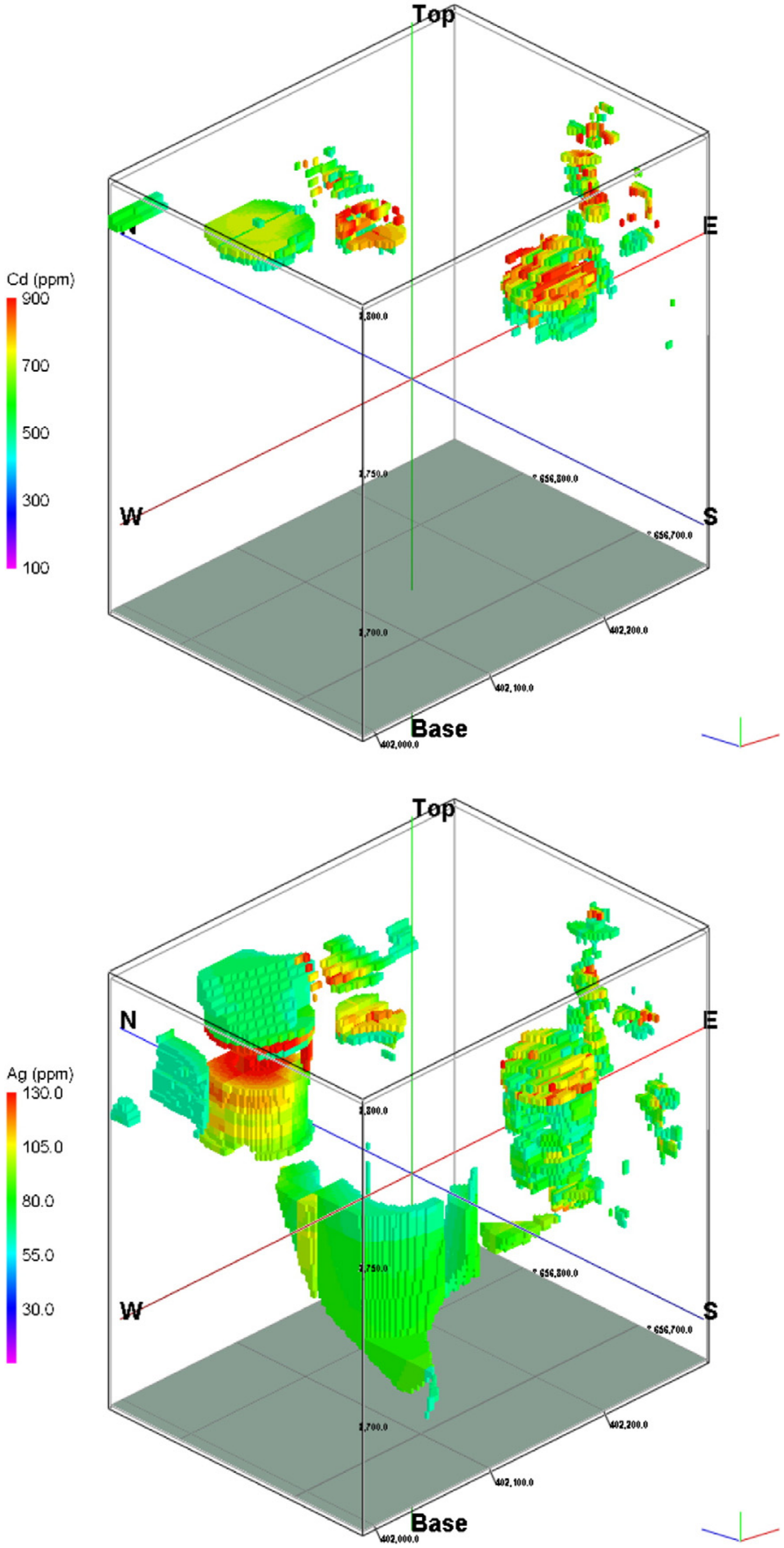

Fig. 4 (*continued*).

transition zone. Elemental ranges for this zone are lower than 7.2%, 1.66%, 30 ppm and 52 ppm for Zn, Pb, Ag and Cd, respectively. This zone is correlated with low sulfidation zone resulting from geological drilling data. Enriched supergene zone is demonstrated in eastern and NE parts of the deposit including Zn, Pb, Ag and Cd grade ranges above 13.8%, 3%, 62 ppm and 407 ppm. These elemental grades are

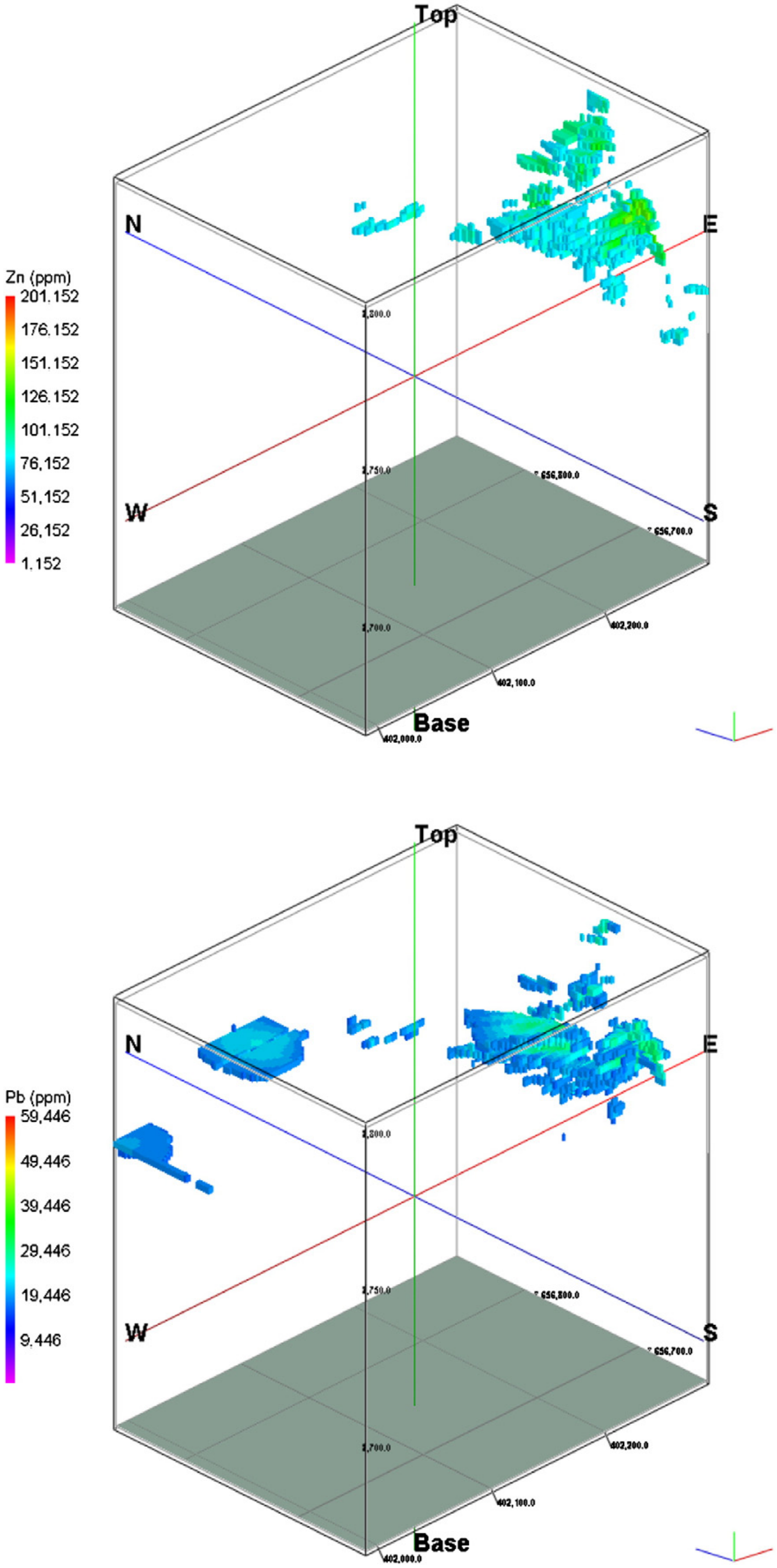

Fig. 5. Hypogene sulfide protore based on C–V method.

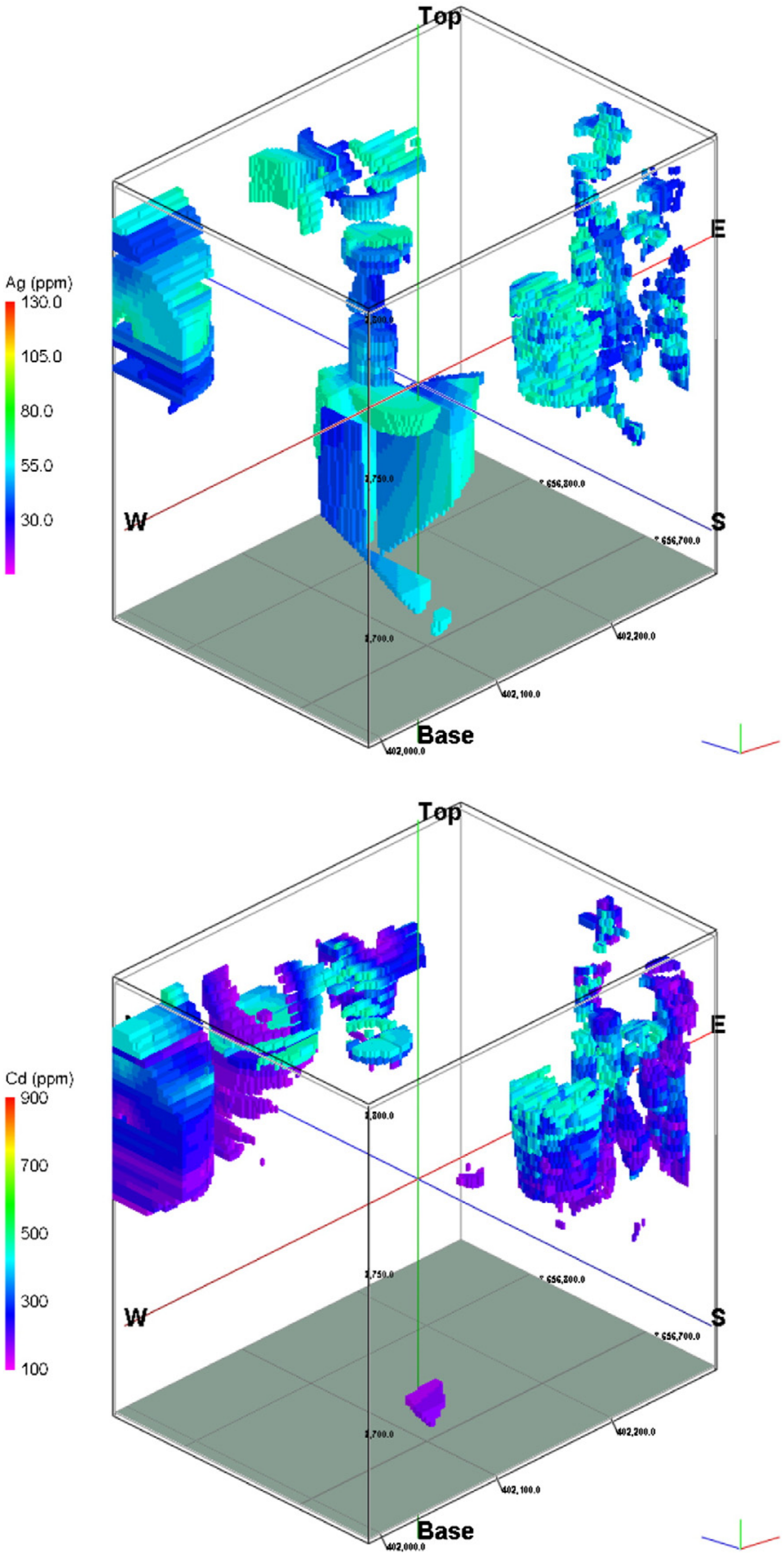

Fig. 5 (*continued*).

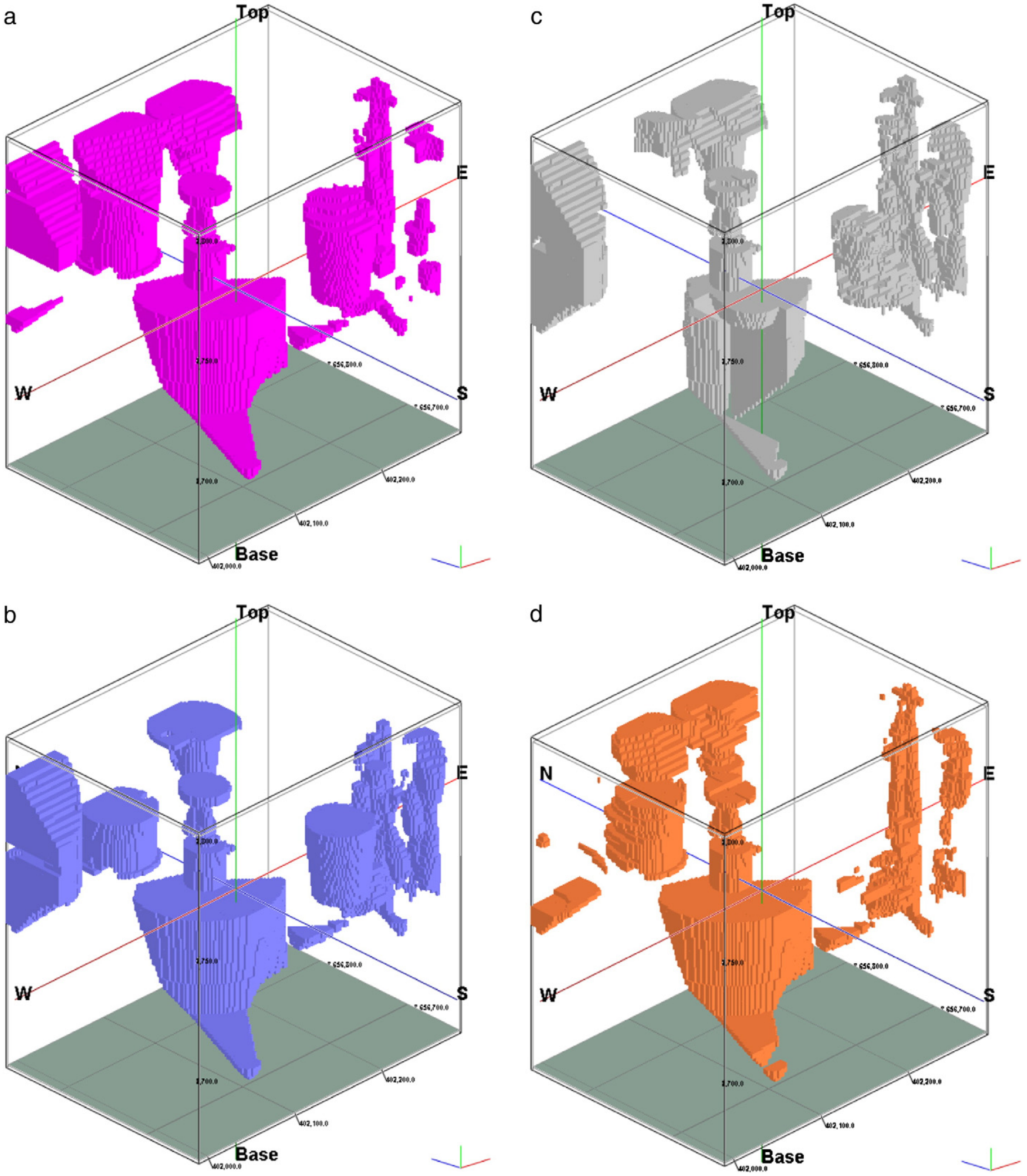

Fig. 6. Low mineralization zone based on C–V model for Zn (a), Pb (b), Ag (c) and Cd (d).

high for Pb–Zn carbonate hosted deposit and this zone is correlated with the oxidation zone obtained from geological data. Hypogene sulfide protore zone resulting from the C–V method consists of Zn between 7.2% and 13.8%, Pb 1.66% and 3%, Ag 30 and 62 ppm and Cd 52 and 407 ppm. There is a noticeable correlation between this zone and the core data, specifically in the eastern and NW parts of the deposit. This means that results obtained from the C–V method are confirmed by geological data, especially core drilling data.

After usage of the C–V fractal method for separation of different mineralization zones in porphyry Cu deposit, based on this research, the C–V

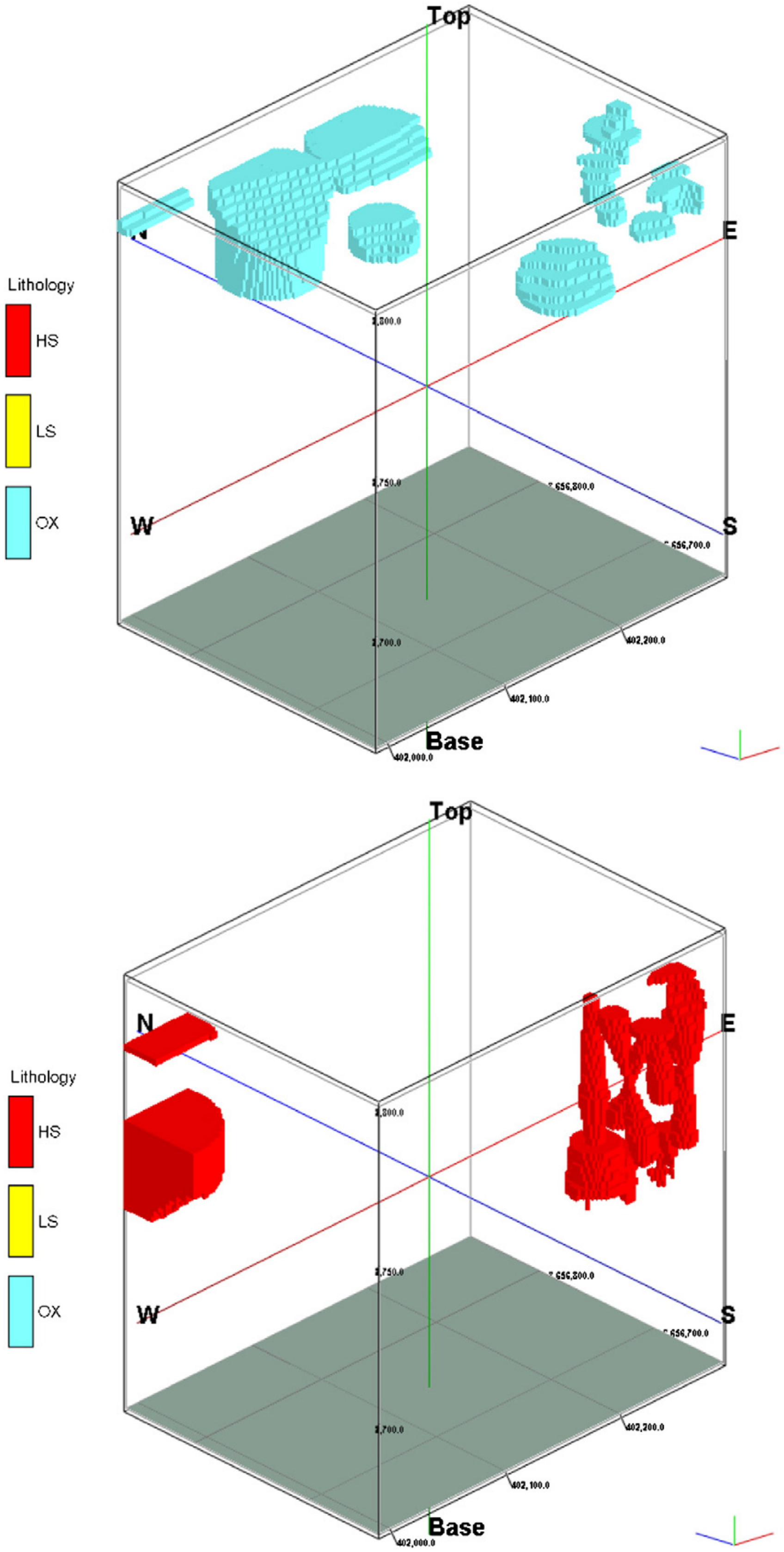

Fig. 7. Zonation model of Tangdezan deposit based on geological logging drilling data.

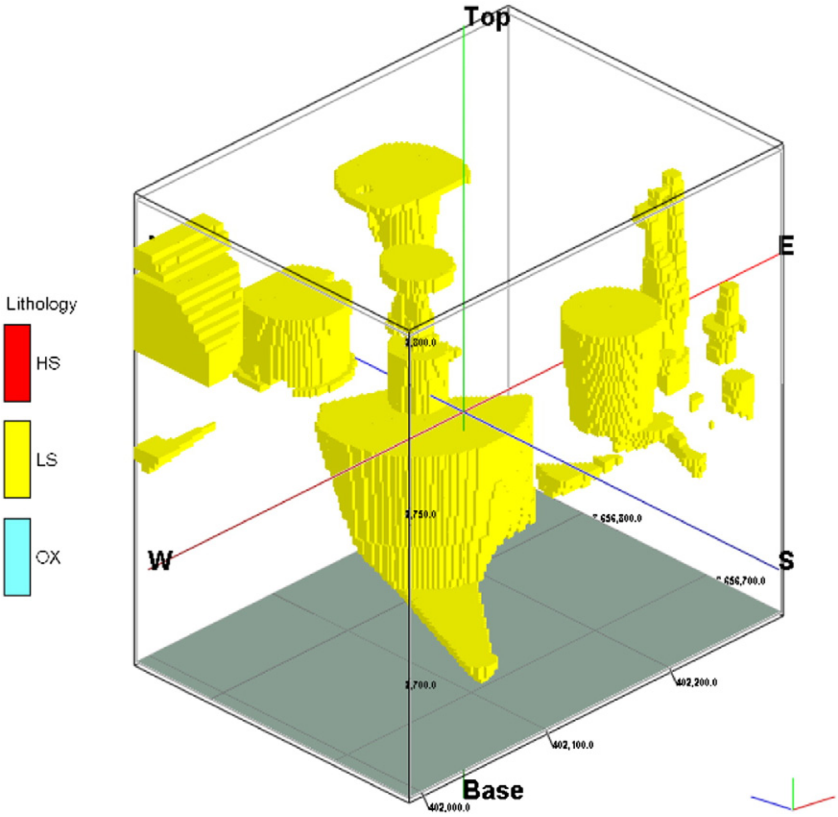

Fig. 7 (*continued*).

method could be applied for separation of mineralization zone in Pb–Zn carbonate hosted deposit.

References

Afzal, P., Khakzad, A., Moarefvand, P., Rashidnejad Omran, N., Esfandiari, B., Fadakar Alghalandis, Y., 2010. Geochemical anomaly separation by multifractal modeling in Kahang (Gor Gor) porphyry system, Central Iran. Journal of Geochemical Exploration 104, 34–46.

Afzal, P., Fadakar Alghalandis, Y., Khakzad, A., Moarefvand, P., Rashidnejad Omran, N., 2011. Delineation of mineralization zones in porphyry Cu deposits by fractal concentration–volume modeling. Journal of Geochemical Exploration 108, 220–232.

Agterberg, F.P., Cheng, Q., Wright, D.F., 1993. Fractal modeling of mineral deposits. In: Elbrond, J., Tang, X. (Eds.), 24th APCOM symposium proceeding, Montreal, Canada, pp. 43–53.

Alavi, M., 1994. Tectonics of Zagros Orogenic belt of Iran, new data and interpretation. Tectonophysics 229, 211–238.

Ali, Kh., Cheng, Q., Zhijun, C., 2007. Multifractal power spectrum and singularity analysis for modelling stream sediment geochemical distribution patterns to identify anomalies related to gold mineralization in Yunnan Province, South China. Geochemistry: Exploration, Environment, Analysis 7 (4), 293–301.

Alldrick, D., Sangster, D., 2005. Mississippi valley- type (MVT) Pb–Zn. Youkan Geological survey.

Bradley, D.C., Leach, D.L., 2003. Tectonic controls of Mississippi Valley-type lead-zinc mineralization in orogenic forelands. Mineralium Deposita 38, 652–667.

Carranza, E.J.M., 2008. Geochemical anomaly and mineral prospectivity mapping in GIS. Handbook of Exploration and Environmental Geochemistry, vol. 11. Elsevier, Amsterdam. 351 pp.

Carranza, E.J.M., 2009. Controls on mineral deposit occurrence inferred from analysis of their spatial pattern and spatial association with geological features. Ore Geology Reviews 35, 383–400.

Cheng, Q., Agterberg, F.P., Ballantyne, S.B., 1994. The separation of geochemical anomalies frombackground by fractalmethods. Journal of Geochemical Exploration 51, 109–130.

Ehya, F., Lotfi, M., Rasa, I., 2010. Emarat carbonate-hosted Zn–Pb deposit, Markazi Province, Iran: A geological, mineralogical and isotopic (S, Pb) study. Journal of Asian Earth Sciences 37, 186–194.

Ghasemi, A., Talbot, C.J., 2006. A new tectonic scenario for the Sanandaj–Sirjan zone (Iran). Journal of Asian Earth Sciences 26, 683–693.

Ghazanfari, F., 1999. Zn–Pb Mines and Deposits in Iran, unpublished report.

Ghazban, F., Mc Nutt, R.H., Schwarcz, H.P., 1994. Genesis of sediment hosted Zn–Pb–Ba deposits in the Irankuh district, Esfahan area, West-Central Iran. Economic Geology 89, 1262–1278.

Ghorbani, M., 2002. An introduction to economic geology of Iran. National Geosciences Database of Iran. Report No. 2, 695 pp. (in Persian).

Ghorbani, M., Tajbakhsh, P., Khoie, N., 2000. Lead and Zinc Deposits in Iran. GSI Book No. 75, 512 pp.

Goncalves, M.A., Mateus, A., Oliveira, V., 2001. Geochemical anomaly separation by multifractal modeling. Journal of Geochemical Exploration 72, 91–114.

Hutchinson, R.W., 1992. Mineral deposits and metallogeny: Indicators of Earth's evolution. In: Schidlowski, M. (Ed.), Early organic evolution: Implications for mineral and energy resources. Springer-Verlag, Berlin Heidenberg, pp. 521–544.

Leach, D.L., Bradley, D., Lewchuk, M.T., Symons, D.T.A., de Marsily, G., Brannon, J., 2001. Mississippi Valleytype lead-zinc deposits through geological time - implications from recent age-dating research. Mineralium Deposita 36, 711–740.

Leach, D.L., Bradley, D.C., Huston, D., Pisarevsky, S.A., Taylor, R.D., Gardoll, S.J., 2010. Sediment-Hosted Lead-Zinc Deposits in Earth History. Economic Geology 105, 593–625.

Li, C., Ma, T., Shi, J., 2003. Application of a fractal method relating concentrations and distances for separation of geochemical anomalies from background. Journal of Geochemical Exploration 77, 167–175.

Mandelbrot, B.B., 1983. The Fractal Geometry of Nature. W. H. Freeman, San Fransisco. 468 pp.

Meshkani, S.A., Mehrabi, B., Yaghubpur, A., Fadakar Alghalandis, Y., 2011. The application of geochemical pattern recognition to regional prospecting: A case study of the Sanandaj–Sirjan metallogenic zone, Iran. Journal of Geochemical Exploration 108 (3), 183–195.

Meyer, C., 1981. Ore-forming processes in geologic history. Economic geology 75th anniversary volume, pp. 6–41.

Momenzadeh, M., 1976. Stratabound lead–zinc ores in the Lower Cretaceous and Jurassic sediments in the Malayer–Esfahan district (west central Iran), lithology, metal content, zonation and genesis. Ph.D. Thesis, Heidelberg University.

Parsgostaran Co., 2010. Exploration report in Tangedezan deposit, Unpublished report.

Reichert, J., 2007. A metallogenetic model for carbonate-hosted non-sulphide zinc deposits based on observations of Mehdi Abad and Irankuh, Central and Southwestern Iran. Ph.D. Thesis, Martin Luther University, Halle Wittenberg.

Reichert, J., Borg, G., 2008. Numerical simulation and a geochemical model of supergene carbonate-hosted non-sulphide zinc deposits. Ore Geology Reviews 33, 134–151.

RockWare Co., 2010. RockWorks 15 manual. www.rockware.com/product/documentation.php?id=165.

Sangameshwar, S.R., Barnes, H.L., 1983. Supergene processes in zinc–lead–silver sulfides ores in carbonates. Economic Geology 78, 1379–1397.

Sangster, D.F., 1990. Mississippi Valley-type and sedex lead-zinc deposits: A comparative examination. Institution of Mining and Metallurgy Transactions 99, B21–B42 (sec. B).

Sangster, D.F. (Ed.), 1996. Carbonate-hosted lead-zinc deposits: Society of Economic Geologists, Special Paper, 4. 687 pp.

Sawkins, F.J., 1984. Metal deposits in relation to plate tectonics. Minerals and Rocks, v. 17. Springer Verlag, Berlin. 325 pp.

Sheikholeslami, R., Bellon, H., Emami, M.H., Sabzehei, M., 2003. Nouvelles données structurales et datations 40K–40Ar sur les roches métamorphiques de la région de Neyriz (zone de Sanandaj–Sirjan, Iran méridional). Leur intérêt dans le cadre du domaine néo-téthysien du Moyen-Orient. Comptes Rendus Geoscience 335, 981–991.

Shelton, K.L., Hagni, R.D., 1993. Geology and geochemistry of Mississippi Valley-type ore deposits. Proceedings Volume. University of Missouri-Rolla, Rolla, Missouri. 195 pp.

Shen, W., Zhao, P., 2002. Theoretical study of statistical fractal model with applications to mineral resource prediction. Computers and Geosciences 28, 369–376.

Sim, B.L., Agterberg, F.P., Beaudry, C., 1999. Determining the cutoff between background and relative base metal contamination levels using multifractal methods. Computers and Geosciences 25, 1023–1041.

Takahashi, T., 1960. Supergene alteration of zinc and lead deposits in limestone. Economic Geology 55, 1084–1115.

Thiele, O., Alavi, M., Assefi, R., Hushmandzadeh, A., Seyed-Emami, K., Zahedi, M., 1968. 1:250000 Golpaygan quadrangle map. Geological survey of Iran.

Turcotte, D.L., 1986. A fractal approach to the relationship between ore grade and tonnage. Economic Geology 18, 1525–1532.

Zuo, R., Cheng, Q., Xia, Q., 2009. Application of fractal models to characterization of vertical distribution of geochemical element concentration. Journal of Geochemical Exploration 102 (1), 37–43.